

## Elastic scattering of $\alpha$ -particles from $^{20}\text{Ne}$

ASHOK KUMAR

Post Graduate Department of Physics, D. B. S. College, Dehra Dun 248 001, India

MS received 17 February 1990; revised 16 July 1990

**Abstract.** A relatively simple procedure using nuclear interaction calculated microscopically from two-nucleon potential employing equivalence of resonating group method and generator coordinate method has been used to calculate the differential cross-sections (DCS) for  $\alpha + ^{20}\text{Ne}$  elastic scattering at  $E_{\text{lab}} = 18.0, 20.2, 21.9, 23.0$  and  $27.2$  MeV. The absorption effects due to the opening of the non-elastic channels are taken into account approximately by the sharp cut-off of lower partial waves. The anomalous large oscillations of the DCS at backward angles at  $E_{\text{lab}} = 18.0$  and  $27.2$  MeV are reproduced. The calculated results are in fair agreement with the experimental data.

**Keywords.**  $\alpha$ -heavy ion elastic scattering; microscopic calculations; absorption effects.

PACS No. 25.60

### 1. Introduction

There has been renewed interest in the elastic scattering of  $\alpha$ -particles from neon nucleus and a few significant experimental and theoretical studies [e.g., Seidlitz *et al* (1958), Cowley and coworkers (Cowley *et al* 1978; Cowley 1979), Abele *et al* (1987); and Ashok Kumar *et al* (1989)] are available to understand the main features such as absorption effects, large oscillations at forward angles and anomalous rise at backward angles in the differential cross-sections (DCS). Seidlitz *et al* (1958) studied the elastic and inelastic scattering of 18 MeV  $\alpha$ -particles from neon. The experimental data for elastic scattering showed pronounced oscillations characteristic of diffraction scattering and also anomalous large angle scattering (ALAS). No exact theory was developed; however, it was found that the DCS are typical of those predicted by previous optical model analyses. Wall (1972) suggested that ALAS is unique to  $\alpha$ -particles and is most clearly observed for target nuclei consisting of multiples of two-neutron and two-proton groups. Thus, this phenomenon was in some way related to the  $\alpha$ -cluster structure of the target and/or the compound nucleus. Several cluster exchange type mechanisms were suggested to describe ALAS, among them heavy particles stripping (Noble and Coelho 1971) and knock-on (Agassi and Wall 1973) were significant. Cowley *et al* (1978) investigated the elastic and inelastic scattering of  $\alpha$ -particles from the stable isotopes of neon. An elastic scattering excitation curve between 26 MeV and 30 MeV taken at backward angles showed a resonance typical of ALAS. The elastic DCS were also measured at 26.2, 27.2 and 27.8 MeV. The results were analysed with a Regge pole plus Woods-Saxon type parametrization of the scattering coefficients (Takeda *et al* 1971). Cowley (1979) made a further study of

elastic scattering of  $\alpha$ -particles from neon and fluctuations in the large-angle excitation functions of the reaction  $^{21}\text{Ne}({}^3\text{He}, \alpha){}^{20}\text{Ne}$  (g.s.). Woods-Saxon optical-potential parameters obtained (Cowley *et al* 1978) from best fits to experimental angular distributions of  $\alpha$ -particles scattered elastically from  ${}^{20}\text{Ne}$  at incident energies of 25.8, 27.0 and 31.1 MeV were used. However, these parameters do not vary systematically as a function of incident energy or target mass and thus this erratic variation of potential parameters suggests that the scattering mechanism of  $\alpha + {}^{20}\text{Ne}$  system is not fully understood by the standard optical model analysis.

Recently Abele *et al* (1987) measured the elastic scattering of  $\alpha$ -particles on some light nuclei in the mass region  $A = 11-24$  (including neon nucleus) at incident energies  $E_\alpha = 48.7$  and 54.1 MeV. The data are analyzed using different phenomenological optical potentials of the Woods-Saxon and Michel type. Special emphasis is laid on the application of the double-folding concept. The imaginary part is expressed in terms of the Fourier-Bessel function. However, DCS for  $\alpha$ - ${}^{20}\text{Ne}$  elastic scattering are measured only at one incident energy, 54.1 MeV. The above studies, which are phenomenological in nature and need a large number of parameters to be systematically adjusted to optimize the fit to the experimental data, are inadequate. To remove this ambiguity some practical microscopic calculations should be carried out using wellknown methods. One such method is the resonating group method (RGM) (Tang *et al* 1978). The important features of the RGM are the utilization of a fully antisymmetric wavefunction, the use of a reasonable nucleon-nucleon potential, and a correct treatment of the total centre-of-mass motion. These features, however, make the RGM calculations quite difficult from a computational viewpoint when the number of nucleons involved is relatively large as in the present case. Accounting for anomalous back-angle scattering and the many reaction channels which open up at higher energies of interest further complicate the matter. It is, therefore, desirable to carry out simplified microscopic calculations which may be valuable for the physical interpretation of the  $\alpha$ -heavy ion scattering data. These data exhibit the effects of large coulomb interaction, transparency for higher partial waves and strong absorption of lower partial waves. In the present investigation a simple microscopic method as described in the previous publication (Ashok Kumar and Srivastava 1988), which accounts for these effects in good approximation, has been applied to calculate the DCS for the  $\alpha + {}^{20}\text{Ne}$  elastic scattering at  $E_{\text{lab}}$  equal to 18.0, 20.2, 21.9, 23.0 and 27.2 MeV. At these energies the experimental data of Seidlitz *et al* (1958) at energy 18.0 MeV, England *et al* (1977) at 20.2, 21.7 and 23.0 MeV and Cowley *et al* (1978) at 27.2 MeV are available with which the calculated results have been compared. Here the effective nuclear potential is taken to be the direct potential of the single-channel RGM scattering equation. Exchange effects are almost neglected while a simple explanation for anomalous large oscillations of the DCS in the back-angle region at  $E_{\text{lab}} = 18.0$  and 27.2 MeV is suggested.

## 2. Formulation

The scattering amplitude,  $f(\theta)$ , for  $\alpha + {}^{20}\text{Ne}$  elastic scattering can be written as,

$$f(\theta) = \frac{1}{2ik} \sum_{l=0}^{\infty} (2l+1) P_l(\cos \theta) \{g(l) \exp[2i(\delta_l + \rho_l)]\}, \quad (1)$$

or

$$f(\theta) = \frac{1}{2ik} \sum_{l=0}^{\infty} (2l+1) P_l(\cos \theta) \exp[2i\rho_l] \{g(l) \exp[2i\delta_l] - 1\} + f_c(\theta), \quad (2)$$

where,  $\delta_l$  are the nuclear phase shifts,  $\rho_l$  and  $f_c(\theta)$  are the coulomb phase shifts and coulomb scattering amplitude respectively. Other symbols have their usual meanings. In the sharp cut-off region of  $l$ -space, the value of reflection coefficient,  $g(l)$ , changes from 0 to 1 in the following manner,

$$g(l) = 0 \text{ for } l < l_c \text{ (complete absorption),}$$

and

$$g(l) = 1 \text{ for } l \geq l_c \text{ (complete transparency).} \quad (3)$$

Classically speaking  $l_c$  represents the sudden transition from no absorption to total absorption of flux at a particular value in  $l$ -space. To understand the role of coulomb and nuclear phase shifts in the elastic scattering, eqs (1) and (2) are analyzed. At small angles  $P_l(-\cos \theta) \sim 1$  so that due to long range of the coulomb force, the series (1) converges slowly; on the other hand in series (2) the term  $\{g(l) \exp[2i\delta_l] - 1\}$  tends rapidly to 0 for  $l \rightarrow \infty$  due to short range of the nuclear force. Conversely, at large angles  $P_l(-\cos \theta) \sim (-1)^l$ , so that the series (1) converges more rapidly than series (2). In a semiclassical picture (Knoll and Schaeffer 1976), this corresponds to the fact that at forward angles the coulomb phase shifts  $\rho_l$  prevail whereas at large angles only nuclear phase shifts  $\delta_l$  contribute significantly to the scattering amplitude.  $\rho_l$  are evaluated by the familiar technique but  $\delta_l$  are calculated with great difficulty from a numerical solution of the following equations,

$$\tan \delta_l = \frac{f_l(R'_m) F_l(\eta', kR'_m) - f_l(R_m) F_l(\eta', kR'_m)}{f_l(R_m) G_l(\eta', R'_m) - f_l(R'_m) G_l(\eta', R_m)}, \quad (4)$$

where

$$\eta' = \frac{\mu z_1 z_2 e^2}{\hbar^2 k}, \quad kR'_m = \frac{(2\mu E)^{\frac{1}{2}} R_m}{\hbar}$$

$R'_m = R_m + \Delta R$  and  $\mu$  is the reduced mass. Also,  $F_l$  and  $G_l$  are the regular and irregular coulomb wavefunctions and are numerically calculated accurately with the help of 'RCWFN Program' of Barnett *et al* (1974).  $f_l(R)$  is calculated from the scattering equation,

$$\frac{d^2 f_l(R)}{dR^2} + \left[ k^2 - \frac{2\mu}{\hbar^2} \left\{ \frac{l(l+1)\hbar^2}{2\mu R} - V_c(R) - V_N(R) \right\} \right] f_l(R) = 0. \quad (5)$$

In the present case there is hardly any overlap of the nuclear charge distributions of the two ions at the energies of interest, thus the coulomb potential is evaluated as

$$V_c(R) = \frac{Z_1 Z_2 e^2}{R}, \quad R \geq (R_1 + R_2). \quad (6)$$

In (6), it would be appropriate to take  $R$  as r.m.s. charge radius,  $R_{\text{ch}}$ , given by

$$\langle R_{\text{ch}}^2 \rangle = \langle R_m^2 \rangle + \langle r_p^2 \rangle, \quad (7)$$

where,  $R_m$  is the r.m.s. matter radius of the nucleus and  $\langle r_p^2 \rangle = 0.64 \text{ fm}^2$ .  $V_N(R)$  in (5) is the effective nuclear potential and here it is taken to be the nuclear part of the direct potential  $V_D(R)$  of the RGM scattering equation when antisymmetrization between nucleons of the two nuclei is neglected. It is given in the double folding form as (Tang *et al* 1978).

$$V_N(R) = \left\langle \Phi_1(\xi_1) \Phi_2(\xi_2) \left| \sum_{\substack{i \in 1 \\ j \in 2}} V_{ij} \right| \Phi_1(\xi_1) \Phi_2(\xi_2) \right\rangle_R. \quad (8)$$

Equation (8) is useful in optical model studies of light ion scattering by medium and heavy-ions. The main reason is that the nucleon-number difference of the interacting nuclei is large which makes the odd-even  $l$ -dependence arising due to Pauli principle insignificant. Here,  $V_{ij}$  is the nuclear part of the two-nucleon interaction given by (Tang *et al* 1978).

$$V_{ij} = [\frac{1}{2}(1 + P_{ij}^\sigma) V_t(ij) - \frac{1}{2}(1 - P_{ij}^\sigma) V_s(ij) + V_R(ij)][\frac{1}{2}u + \frac{1}{2}(2 - u)P_{ij}^r], \quad (9)$$

where

$$V_R(ij) = V_{0R} \exp[-k_R(\mathbf{r}_i - \mathbf{r}_j)^2], \quad V_t(ij) = -V_{0t} \exp[-k_t(\mathbf{r}_i - \mathbf{r}_j)^2],$$

$$V_s = -V_{0s} \exp[-k_s(\mathbf{r}_i - \mathbf{r}_j)^2], \quad (10)$$

$$V_{0R} = 200.0 \text{ MeV}, \quad k_R = 1.487 \text{ fm}^{-2}, \quad V_{0t} = 178.0 \text{ MeV}, \quad k_t = 0.639 \text{ fm}^{-2},$$

$$V_{0s} = 91.85 \text{ MeV}, \quad k_s = 0.465 \text{ fm}^{-2}, \quad (11)$$

where,  $P_{ij}^r$  and  $P_{ij}^\sigma$  are the space- and the spin-exchange operators.  $V_t$ ,  $V_s$  and  $V_R$  are the two-nucleon triplet, singlet and repulsive interactions, respectively. Equation (9) is particularly chosen because it yields a satisfactory description of not only the two nucleon low-energy scattering data but also the essential properties of the deuteron, triton and  $\alpha$ -particles. The exchange-mixture parameter  $u$  is an adjustable parameter in the calculation. Its value is determined by fitting the light-ion separation energy in the lowest  $l = 0$  state of the compound nucleus. For example, in the  $\alpha + {}^{16}\text{O}$  case, one adjusts  $u$  until the calculation yields the experimental value (Ajzenberg-Selove 1972) of 4.73 MeV for the  $\alpha$ -particle separation energy in the ground state of  ${}^{20}\text{Ne}$ . This adjustment is essential because various simplifications are made in the present calculation. The resultant value of  $u$  so determined should be reasonably close to 1 which corresponds to a Serber exchange. In case the value of  $u$  comes out to be much different from 1 then adjusting  $u$  is a crude procedure and a detailed calculation will be desirable (Tang *et al* 1978). Thus, in the present calculation  $u$  is simply varied close to 1 to get best experimental fits for DCS (Ashok Kumar and Srivastava 1988). Now using the equivalence relations between the RGM and the generator coordinate method (GCM) (Kamimura and Matsuse 1974),  $V_N(R)$  can be written as

$$V_N(R) = \frac{1}{(2\pi)^3} \int d\mathbf{K} \exp(-i\mathbf{K} \cdot \mathbf{R}) \exp(K^2/8\eta) \int d\mathbf{S} \exp(i\mathbf{K} \cdot \mathbf{S}) V_D(\mathbf{S}), \quad (12)$$

where,

$$\eta = \frac{A_1 A_2}{2(A_1 + A_2)} \omega \quad (13)$$

$A_1$  and  $A_2$  are the mass numbers of the colliding nuclei.  $\omega$  is the width parameter for the harmonic oscillator orbitals used in the Slater determinant wavefunctions and  $V_D(\mathbf{S})$  is given by

$$V_D(\mathbf{S}) = 2X_d \sum_{k,l} \int \Phi_k^*(\mathbf{r}_1 - \mathbf{S}_1) \Phi_l^*(\mathbf{r}_2 - \mathbf{S}_2) U(r_{12}) \Phi_k(\mathbf{r}_1 - \mathbf{S}_1) \times \Phi_l(\mathbf{r}_2 - \mathbf{S}_2) d\mathbf{r}_1 d\mathbf{r}_2 \quad (14)$$

In (14),  $\Phi_k$  and  $\Phi_l$  denote the harmonic oscillator orbitals  $k$  and  $l$  of nuclei 1 and 2 centred around  $\mathbf{S}_1$  and  $\mathbf{S}_2$ , respectively,  $U(r_{12})$  is the radial part of the two-nucleon interaction and

$$X_d = 2(4w - m + 2b - 2h). \quad (15)$$

Here  $w$ ,  $m$ ,  $b$  and  $h$  are the familiar Wigner, Majorana, Bartlett and Heisenberg exchange mixture parameters, respectively. The values of these parameters are determined in (20). An apparently important point in folding model analyses is the treatment of the absorption effects by the imaginary part of the optical potential. Several forms of the imaginary part of the standard Woods-Saxon potential were used in the past. Nevertheless, it is understood that once the real part of the optical potential has been obtained independently then just using different standard forms of the imaginary potential do not further improve the fit to the scattering data because the imaginary potential is well determined only in a limited radial region (Gils 1987). Thus, an imaginary potential can be approximated easily without much loss in accuracy and in the present calculation classical sharp cut-off procedure is used for absorption effects. According to it  $l_c$  in (3) corresponds to the partial wave for which the maximum of the total interaction is equal to the c.m. incident energy in the surface region at  $R = R_c$ .

It is seen that  $\alpha$ - ${}^{20}\text{Ne}$  elastic scattering study exhibits enhancement and pronounced oscillatory structure of the DCS at backward angles  $>90^\circ$  particularly at incident energies of 18.0 and 27.2 MeV. Since the conventional potentials of Woods-Saxon form fail to explain this strange feature, its explanation is sought outside the domain of the standard optical model. It has been investigated by many authors, e.g., Michel and Vanderpoorten (1977), Gubler *et al* (1978, 1981), Love (1978), Kiebele *et al* (1978) and Abele *et al* (1987) that the folding potential model supplemented by an adjustable imaginary potential provided a satisfactory description of elastic  $\alpha$ -nucleus scattering over the full angular range with special attention to the large angle anomaly. In the similar manner it has been investigated in our recent work (Ashok Kumar *et al* 1989) that the double folding model supplemented by sharp cut-off procedure for absorption is capable of explaining the so-called anomalous large angle oscillations of the DCS in the  $\alpha + {}^{20}\text{Ne}$  system. Further, exchange effects arise from antisymmetrization of the target and projectile coordinates. Since  $\alpha$ -particle is taken as an elementary particle with a large binding energy and a small radius, it is considered to be distinguishable from the nucleons of the target (Lassaut 1981). Moreover, by studying the cross-section or phase-shift behaviour (Le Mere *et al* 1982) it is noted that many exchange terms are only of minor significance when the absorption is strong as in the present case. Hence, no appreciable exchange effects are considered here and they are very crudely accounted by varying  $u$  with energy.

### 3. Calculation

For calculation of  $V_N(R)$ , the projectile and target nuclei are chosen to have  $(1s)^4$  and  $(1s)^4(1p)^{12}(2s)^4$  configurations, respectively. The configuration of  $^{20}\text{Ne}$  is considered to be that of a closed shell with zero spin and magnetic moment (Roy and Nigam 1967). This particular configuration yields a spherically symmetric form for  $V_N(R)$  while the usual configuration  $(1s)^4(1p)^{12}(2s, 1d)^4$  will lead to non-spherical form causing complexities in the calculations. The choice of a closed shell configuration for  $^{20}\text{Ne}$  is reasonable because for nuclei immediately beyond  $^{16}\text{O}$ , both the  $1d_{5/2}$  and the  $2s_{1/2}$  levels are available for the valence nucleons and are close enough compared to the interaction matrix elements between them (de Shalit and Feshbach 1974). Thus, final results are not expected to be sensitive to this choice. The calculations would be simplified if one chooses a common oscillator width parameter  $\omega$  for both the non-identical nuclei  $\alpha$  and  $^{20}\text{Ne}$ . This will ensure correct treatment of centre-of-mass motion (Friedrich *et al* 1976). Thus the value of  $\omega$  employed here is  $0.3460 \text{ fm}^{-2}$ . It is the mean of the individual  $\omega$ -values  $0.514 \text{ fm}^{-2}$  and  $0.3124 \text{ fm}^{-2}$  for  $\alpha$  and  $^{20}\text{Ne}$ , respectively, which yield the experimentally determined r.m.s. matter radii for the respective nuclei (Ripka 1967). Hence, the translationally invariant harmonic-oscillator shell-model wavefunctions of lowest configurations with common width parameter  $\omega$  for  $\alpha$  and  $^{20}\text{Ne}$  are as follows,

$$\begin{aligned}\Phi_{04} &= A_{04} \left[ \prod_{i=1}^4 h_i(\mathbf{r}_i - \mathbf{R}_{04}) \Omega_i(s_i, t_i) \exp \left\{ -\frac{\omega}{2} (\mathbf{r}_i - \mathbf{R}_{04})^2 \right\} \right], \\ \Phi_{20} &= A_{20} \left[ \prod_{i=1}^{20} h_i(\mathbf{r}_i - \mathbf{R}_{20}) \Omega_i(s_i, t_i) \exp \left\{ -\frac{\omega}{2} (\mathbf{r}_i - \mathbf{R}_{20})^2 \right\} \right],\end{aligned}\quad (16)$$

where,  $A_{04}$  and  $A_{20}$  are four-nucleon and twenty-nucleon antisymmetrization operators, respectively, while  $\mathbf{R}_{04}$  and  $\mathbf{R}_{20}$  denote the centre-of-mass (c.m.) coordinates of  $\alpha$  and  $^{20}\text{Ne}$  given by

$$\mathbf{R}_{04} = \frac{1}{4} \sum_{i=1}^4 \mathbf{r}_i \quad \text{and} \quad \mathbf{R}_{20} = \frac{1}{20} \sum_{i=1}^{20} \mathbf{r}_i, \quad (17)$$

where  $\mathbf{r}_i$  being the spatial coordinates of the  $i$ th nucleon. The functions  $h_i$  being the polynomials in single-particle spatial coordinates and the spin-iso spin functions  $\Omega_i(s, t)$  are given by

$$\begin{aligned}\Omega_i(s, t) &= \alpha(s)\pi(t) \quad \text{for } i = 1, 5, 9, 13, 17 \\ &= \alpha(s)\nu(t) \quad \text{for } i = 2, 6, 10, 14, 18 \\ &= \beta(s)\pi(t) \quad \text{for } i = 3, 7, 11, 15, 19 \\ &= \beta(s)\nu(t) \quad \text{for } i = 4, 8, 12, 16, 20,\end{aligned}\quad (18)$$

where  $\alpha(s)$ ,  $\beta(s)$ ,  $\pi(t)$  and  $\nu(t)$  denote the spin-up, spin-down, isospin-up and isospin-down functions, respectively. Now using (9) to (15),  $V_N(R)$  is calculated as

$$V_N(R) = \sum_{n=1}^3 G_n \exp[-F_n R^2] \{A_n + B_n R^2 + C_n R^4\},$$

where

$$\begin{aligned}
 G_n &= -\frac{X_{dn} V_{0n}}{3} \left[ \frac{10\omega}{10\omega + 17k_n} \right]^{3/2}, \\
 F_n &= \frac{10\omega k_n}{(10\omega + 17k_n)}, \\
 A_n &= 30 \left\{ 1 - \frac{20k_n(5\omega + 6k_n)}{(10\omega + 17k_n)^2} \right\}, \\
 B_n &= \left\{ \frac{2000\omega k_n^2(10\omega + 7k_n)}{(10\omega + 17k_n)^3} \right\}, \\
 C_n &= \left\{ \frac{40000\omega^2 k_n^4}{(10\omega + 17k_n)^4} \right\}, \tag{19}
 \end{aligned}$$

and

$$X_{dn} = 2(4w_n - m_n + 2b_n - 2h_n)$$

with

$$w_1 = b_1 = w_2 = -b_2 = \frac{1}{4}u,$$

$$m_1 = h_1 = m_2 = -h_2 = \frac{1}{4}(2 - u),$$

$$w_3 = \frac{1}{2}u, m_3 = \left( \frac{2 - u}{2} \right),$$

$$b_3 = h_3 = 0, k_1 = k_t, k_2 = k_s, k_3 = k_R,$$

$$V_{01} = V_{0t}, V_{02} = V_{0s} \text{ and } V_{03} = V_{0R}. \tag{20}$$

The coulomb potential was calculated from (6) with  $z_1 = 2$ ,  $z_2 = 10$ ,  $R_1 = 1.888$  fm and  $R_2 = 3.211$  fm.

Then at the incident energy of interest, the values of  $l_c$  and  $R_c$  were numerically obtained as described in §2. The value of  $u$  is also varied around 1 for best results. The required coulomb phase shifts were easily obtained and the nuclear phase shifts were numerically calculated from (4) and (5). Then  $f(\theta)$  is obtained from (1) by changing the upper limit of  $\infty$  with a finite value  $l_{\max}$  for which  $\delta_{l_{\max}}$  was nearly zero. Thus, the DCS ( $\sigma(\theta)$ ) were obtained from the relation,

$$\sigma(\theta) = |f(\theta)|^2. \tag{21}$$

The calculated values of  $u$ ,  $l_c$ ,  $l_{\max}$  and  $R_c$  at five incident energies are given in table 1.

**Table 1.** Calculated values of  $l_c$ ,  $l_{\max}$  and  $R_c$  for  $\alpha + {}^{20}\text{Ne}$  elastic scattering.

$E_{\text{lab}}(\text{MeV})$	$u$	$l_c$	$l_{\max}$	$R_c(\text{fm})$
18.0	0.9	08	15	5.89
20.2	0.9	09	16	5.69
21.9	1.0	10	17	5.89
23.0	1.0	10	17	5.89
27.2	1.0	11	19	5.59

#### 4. Results and discussion

The calculated DCS,  $\sigma(\theta)$  at  $E_{\text{lab}} = 20.2, 21.9$  and  $23.0$  MeV are shown by solid-line curves in figure 1. The ratios of  $\sigma(\theta)$  to the corresponding Rutherford cross-section, ( $\sigma_R$ ), at  $E_{\text{lab}} = 18.0$  and  $27.2$  MeV are also shown by solid-line curves in figure 2. The experimental data of Seidlitz *et al* (1958) at  $18.0$  MeV, England *et al* (1977) at  $20.2, 21.9$  and  $23.0$  MeV and Cowley *et al* (1978) at  $27.2$  MeV are shown by solid circles over full angular range in figures 1 and 2. The agreement between calculated results and the experimental data at  $18.0$  MeV is fairly good, while it is fair at  $20.2, 21.9$  and  $23.0$  MeV, respectively. However, at  $27.2$  MeV, the agreement is poor over the whole angular range. The energies above  $27.2$  MeV are thus not considered in the present investigation. It may be pointed out that no special attention has been given to explain the back-angle scattering, even though when fitting the forward-angle data only, this model predicts a reasonable correct pattern for the backward cross-sections. As an example, the upper solid-line curve in figure 2 represents a fit to  $18.0$  MeV data for  $\theta < 80^\circ$ . This fit not only describes the data for  $\theta < 80^\circ$  but also the anomalous large oscillations of the angular distributions for  $\theta > 120^\circ$  rather well. However, it is only

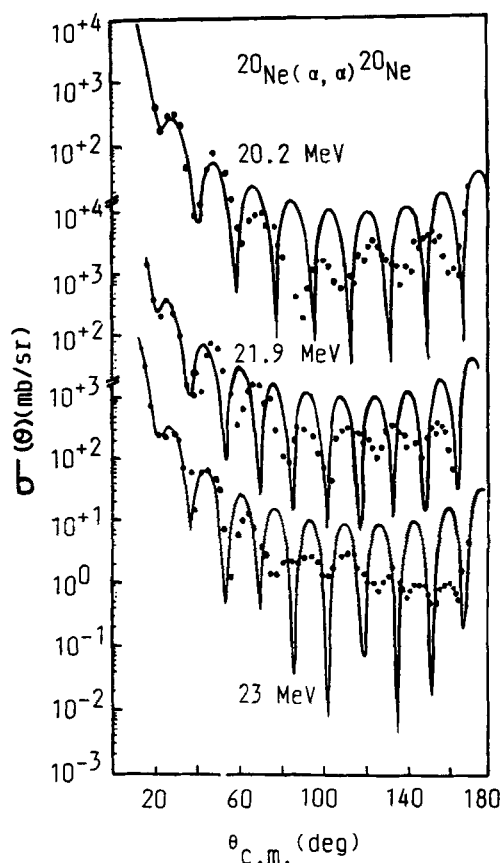


**Figure 1.** The calculated DCS ( $\sigma(\theta)$ ) for  $\alpha + {}^{20}\text{Ne}$  elastic scattering at  $E_{\text{lab}} = 20.2, 21.9$  and  $23.0$  MeV as a function of  $\theta_{\text{c.m.}}$  (deg.) are shown by solid-line curves along with the experimental data of England *et al* (1977) shown by solid circles.

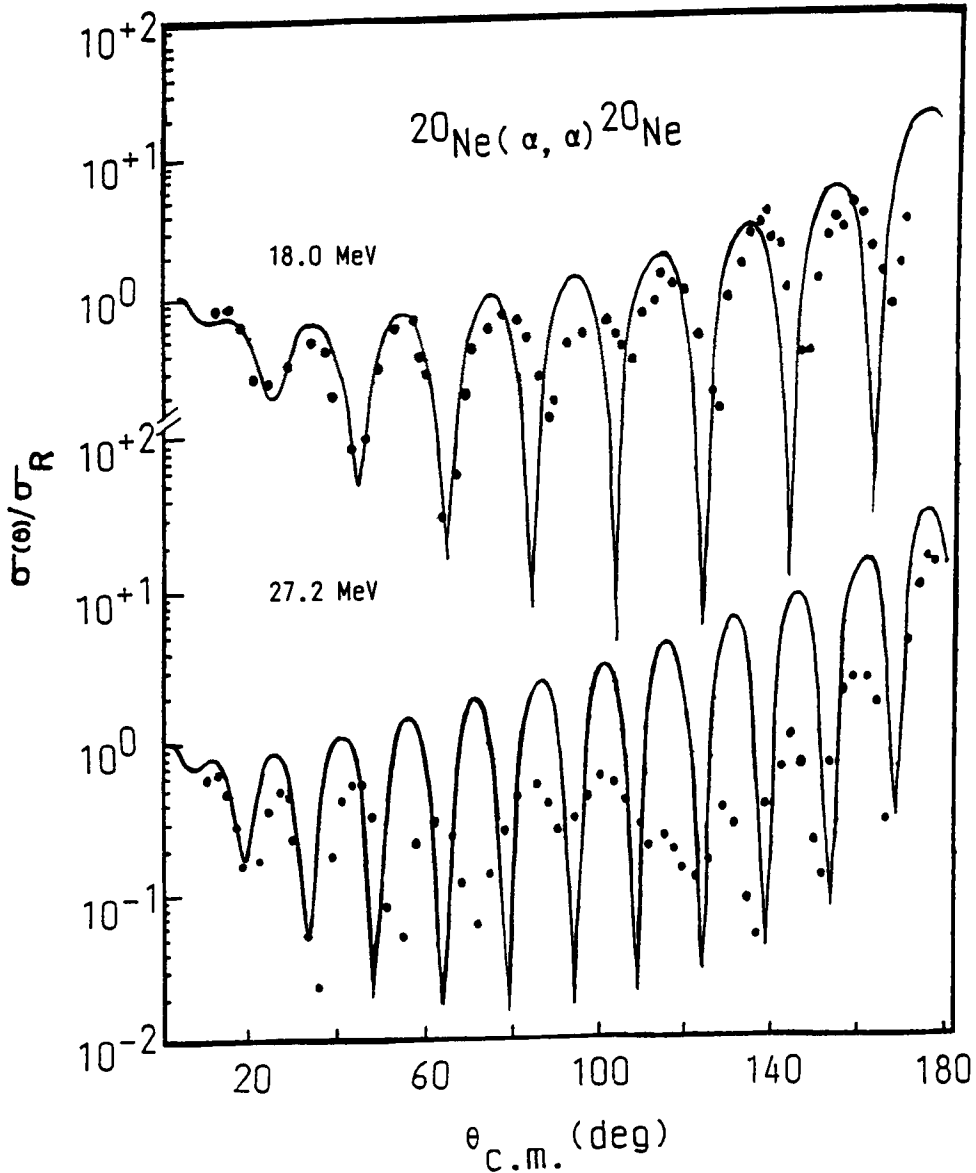


**Figure 2.** The ratios of the calculated DCS ( $\sigma(\theta)$ ) and the Rutherford cross-section ( $\sigma_R$ ) for  $\alpha + {}^{20}\text{Ne}$  elastic scattering at  $E_{lab} = 18.0$  and  $27.2$  MeV as a function of  $\theta_{c.m.}$  (deg.) are shown by solid-line curves along with the experimental data of Seidlitz *et al* (1958) and Cowley *et al* (1978), respectively, shown by solid circles.

fair at intermediate angles. This behaviour occurs also at  $27.2$  MeV and shown by lower solid-line curve in figure 2 but the back-angle agreement is not as striking as in the former case. Further, all the solid-line curves show sharp oscillations for almost over the whole angular range in accordance with the experimental data. In general, it may be said that in each case the agreement is much better at smaller angles than that at the larger angles. Nevertheless, at higher energies the quality of the agreement progressively deteriorates, suggesting some improvements to be incorporated.

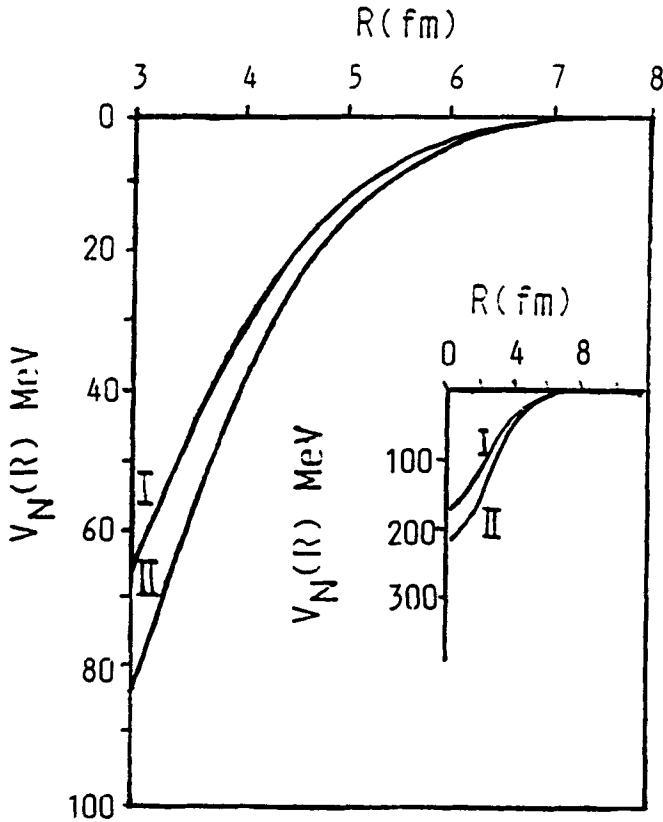


**Figure 3.** The radial dependence of the calculated real nuclear potential,  $V_N(R)$ , for  $\alpha + {}^{20}\text{Ne}$  system is shown by solid-line curves I and II for  $u = 0.9$  and  $1.0$ , respectively.

The exchange effects, which cause the ion-ion potential to be energy-dependent and non-local, are almost neglected. Consequently, if one wants to get some crude idea of exchange effects in the present model then one has to allow for variation of  $u$  around 1, which appears in the energy-independent  $V_N(R)$ , w.r.t energy [see (9) and (12)]. For this purpose the best visual agreements were obtained for the values of  $u = 0.9$  at 18.0 and 20.2 MeV and  $u = 1.0$  at 21.9, 23.0 and 27.2 MeV, respectively. These values of  $u$  are either 1 or close to 1 as desired. It appears that the value of  $u$  also increases with increase in incident energy. The variation of  $V_N(R)$  was computed as a function of  $R$  using (12) at  $u = 0.9$  and  $1.0$  and are shown by solid-line curves I and II, respectively, in figure 3. Curves I and II suggest that deeper  $V_N(R)$  is required for higher incident energies as expected from the decreasing role played by the Pauli principle effects (Sartor *et al* 1981). It is also evident that shape of  $V_N(R)$  does not resemble the Woods-Saxon potential. It is quite deep at small separations and decreases much faster than like a simple exponential as in the Woods-Saxon type potential. These findings agree with the conclusions of Satchler and Love (1979) regarding the form of folded potentials.

Hence, in the present investigation a good estimate of DCS over full angular range for  $\alpha + {}^{20}\text{Ne}$  system at incident energies much above the coulomb barrier  $E_B (\approx 5.58 \text{ MeV})$  is obtained with relatively little amount of computation. Further, this approach is direct and based on simple assumptions and thus gives a better

physical insight about the elastic scattering mechanism. Also  $V_N(R)$  is derived microscopically on the basis of fundamental two-nucleon potential and it overcomes the shortcomings of the phenomenological optical potentials. It is worth mentioning that the two-nucleon potential of the present investigation has been used in many RGM calculations yielding satisfactory results (Tang *et al* 1978). Unlike the Woods-Saxon potential no large variations of different parameters are involved. However, it is seen that the sharp cut-off procedure is a very simplified approximation for absorption effects especially at higher energies. Consequently a better approach for the imaginary potential is desirable and anomalous back-angle scattering will then get a proper explanation. Thus for more definite conclusions it is essential to carry out modified analyses for other alpha-heavy ion systems. A few systems are under investigation.

## References

- Abele H, Hauser H J, Korber A, Leitner W, Neu R, Plappert H, Rohwer T, Staudt G, Straber M, Walz M, Welte S, Eversheim P D and Hinterberger F 1987 *Z. Phys.* **A326** 373
- Agassi D and Wall N S 1973 *Phys. Rev.* **C7** 1368
- Ajzenberg-Selove F 1972 *Nucl. Phys.* **A190** 1
- Ashok Kumar and Srivastava B B 1988 *Can. J. Phys.* **66** 813
- Ashok Kumar, Bhatnagar V K and Sharma O D 1989 *Proc. of Symp. on Nucl. Phys. India* **B32** 043
- Barnett A R, Feng D H, Steed J W and Goldfarb L J B 1974 *Comput. Phys. Commun.* **8** 377
- Cowley A A, Vanstaden J C, Mills S J and Cronje P M 1978 *Nucl. Phys.* **A301** 429
- Cowley A A 1979 *Nucl. Phys.* **A325** 83
- deShalit Amos and Feshbach H 1974 *Theor. Nucl. Phys.* (John Willey and Sons) **1** 362
- England J B A, Casal E, Garcia A, Picazo T, Aguilar J and SenGupta H M 1977 *Nucl. Phys.* **A284** 29
- Friedrich H, Langanke K and Weiguny A 1976 *Phys. Lett.* **B63** 125
- Gils H J 1987 *Nucl. Phys.* **A473** 111
- Gubler H P, Kiebele U, Meyer H O, Plattner G R and Sick I 1978 *Phys. Lett.* **B74** 202
- Gubler H P, Kiebele U, Meyer H O, Plattner G R and Sick I 1981 *Nucl. Phys.* **A351** 29
- Kamimura M and Matsuse T 1974 *Prog. Theor. Phys.* **51** 438
- Kiebele U, Baumgartner E, Gubler H P, Meyer H O, Plattner G R and Sick I 1978 *Helv. Phys. Acta* **51** 726
- Knoll J and Schaeffer 1976 *Ann. Phys. (NY)* **97** 307
- Lassaut M 1981 *Phys. Lett.* **B105** 252
- Le Mere M, Fujiwara Y and Tang YC 1982 *Phys. Rev.* **C26** 1847
- Love W G 1978 *Phys. Rev.* **C17** 1876
- Michel F and Vanderporten R 1977 *Phys. Rev.* **C16** 142
- Noble J and Coelho H 1971 *Phys. Rev.* **C3** 1840
- Ripka G 1967 in *Fundamentals in Nuclear Theory* (eds) A deShalit and C Villi (Vienna: International Atomic Energy Agency)
- Roy R R and Nigam B P 1967 *Nuclear Physics*, (John Willey and Sons) 245
- Sartor R, Faessler A, Khadkikar S B and Krewald S 1981 *Nucl. Phys.* **A359** 467
- Satchler G R and Love W G 1979 *Phys. Rep.* **53** 183
- Seidlitz L, Bleuler E and Tendam D J 1958 *Phys. Rev.* **110(3)** 682
- Takeda M, Kato S and Yamazaki T 1971 *J. Phys. Soc. Jpn.* **31** 625
- Tang Y C, Le Mere M and Thompson D R 1978 *Phys. Rep.* **43(3)** 167
- Wall N S 1972 *Proc. of Symp. on Four-Nucleon Correlations and Alpha Rotator Structure* (Marburg) (ed.) R Stock p. 115